

INTERFEROMETRIC OBSERVATORIES IN EARTH ORBIT

I. I. Hussein¹, D. J. Scheeres², D. C. Hyland³

The University of Michigan

Ann Arbor, MI 48109-2140

February 11, 2003

Abstract

We propose a class of satellite constellations that can act as interferometric observatories in Low Earth Orbit (LEO), capable of forming high resolution images in time scales of a few hours without the need for active control. First we discuss the requirements to achieve these imaging goals. Next we define a class of constellations that can achieve these goals in LEO. An optimization procedure is also defined that supplies m pixels of resolution with a minimum number of satellites. For the example considered, this procedure results in an observatory that is within 0-2 satellites from a lower bound of \sqrt{m} satellites. We introduce a linear imaging constellation and formulate a concise 0-1 mathematical program, the solution of which is the solution to optimal aperture configuration for full coverage of the wave number plane. Next, we extend the LEO observatory to a general Earth orbit and relate the solution of the (linear array) 0-1 program to that of the Earth orbiting constellation. We discuss how the zonal J_2 effect can be utilized to scan the observatory across the celestial sphere and, finally, we discuss some practical implementation issues.

1 Introduction to the Imaging Requirements

Interferometric imaging is performed by measuring the mutual intensity (the two point correlation¹) that results from the collection and subsequent interference of two electric field measurements of a target made at two different observation points. While

¹PhD Candidate, Aerospace Engineering, ihussein@umich.edu

²Associate Professor of Aerospace Engineering, scheeres@umich.edu

³Professor of Aerospace Engineering, dhiland@engin.umich.edu

moving relative to each other, the satellites collect and transmit these measurements, which are later combined at a central node using precise knowledge of their locations and timing of data collection. A least squares error estimate of the image can be reconstructed given the mutual intensity measurements, parameters of the optical system, and the physical configuration of the observatory. To assess the quality of the reconstructed image, the reconstructed image is Fourier transformed into a two dimensional plane of spatial frequencies (the wave number plane). At any given point on the wave number plane, the modulation transfer function (MTF) is defined as the ratio of the estimated intensity to the true image intensity. For an interferometric imaging constellation the MTF can be computed given the measurement history and corresponding relative position data among the light collecting spacecraft. In the wave number plane, a point with a zero MTF value implies that the system is “blind” to the corresponding sinusoidal pattern, while a large value of the MTF implies that the image signal can be restored at that wave number via an inverse Fourier transform^{1,2}. The MTF, as a measure of the imaging system’s performance, is a function of both the optical system and the configuration of the observatory in physical space. In this note we address the issue of designing the configuration of an interferometric observatory that ensures a non-zero value of the MTF within a desired region in the wave number plane.

For a general satellite constellation, denote the position vector of satellites i and j by \mathbf{R}_i and \mathbf{R}_j , respectively, $i, j = 0, 1, \dots, N - 1$, where N is the number of satellites. Let $\mathbf{R}_{ij} = \mathbf{R}_j - \mathbf{R}_i$ be the relative position vector between satellites i and j and \mathbf{r}_{ij} be the projection of \mathbf{R}_{ij} onto a plane perpendicular to the line of sight of the observatory. Let \bar{z} be the distance from the image plane to the observation plane. Denote by the term “picture frame” the angular extent of the intended image on the image plane. The picture frame has a diameter of length \bar{L} . Pixelating the image plane into an $m \times m$ grid, the size of each pixel is $L = \bar{L}/m$, and the resulting angular resolution is $\theta_r = L/\bar{z}$. Additionally, the angular extent of the desired picture frame is given by $\theta_p = \bar{L}/\bar{z}$, leading to $\theta_p = m\theta_r$.

Dimensions of features in the wave number plane are the reciprocals of the corresponding dimensions in the physical plane. Thus the resolution disc is a disc of diameter $1/\theta_r$ and is the region where we desire the MTF to have nonzero values (henceforth, simply denoted by wave number plane coverage). The picture frame region is a circular disc of diameter $1/\theta_p$. Therefore, the diameter of the resolution disc is m times the diameter of the picture frame disc in the wave number plane (see Figure (1)). As the relative position vector of two spacecraft varies in the physical plane, the picture frame disc moves in the wave number plane, where its center follows the trajectory of the vector given by $\pm \mathbf{r}_{ij}/\lambda$, where λ is the imaging wavelength of interest. Each satellite, by itself, will contribute a disc that is centered at the origin with a diameter of $1/\theta_p$, and each pair of satellites will contribute two discs of diameter $1/\theta_p$ located 180 degrees apart with a radius of $\frac{r_{ij}}{\lambda}$ from the center, where $r_{ij} = |\mathbf{r}_{ij}|$. Define the minimum relative distance between satellites to be $d_{\min} = \lambda/\theta_p$. To completely cover the resolution disc in the wave number plane it is sufficient to

have satellites distributed such that there exist pairs with relative distances d_{\min} , $2d_{\min}$, \dots , $\frac{1}{2}(m-1)d_{\min}$. Let $d_{\max} = \frac{1}{2}(m-1)d_{\min}$.

2 Circular Orbit Constellations

We propose a class of very long baseline constellations that achieves the requirement that the wave number plane be completely covered. The satellite constellation is placed on a circular arc that is a segment of a low Earth orbit and whose center is located at the center of the Earth (see Figure (1)). The satellites are distributed such that the second satellite is located at a distance of d_{\min} from the first satellite, the third at $2d_{\min}$ from the first, the fourth at $3d_{\min}$ from the first, and so on. Thus, a constellation of N_f satellites will have the N^{th} satellite located at a distance of $(N-1)d_{\min}$ from the first. This distribution, defined as the ‘‘fundamental’’ constellation, implies that there are $m = 2N_f - 1$ pixels and ensures the complete coverage of the wave number plane, once the constellation is rotated 180° (i.e. after half an orbit period). Figure (1) shows the geometry of this configuration for $N_f = 3$ satellites ($m = 5$ pixels). We nominally assume that the orbit plane is perpendicular to the line of sight to the target.

To compute the precise locations of the satellites in the constellation, specify wavelength of interest, λ , and the desired angular extent of the picture frame $\theta_p = \bar{L}/\bar{z}$. Given a number of satellites N_f , or the number of pixels m , one then obtains the corresponding angular resolution, θ_r , and knowledge of θ_p enables us to compute d_{\min} and d_{\max} . Throughout this note we use the following values: $\lambda = 10\mu\text{m}$, $\bar{z} = 7.408 \times 10^{14}\text{km}$ (~ 24 parsec from the Earth), $\bar{L} = 13 \times 10^3\text{km}$, $r_o = 7,200\text{km}$ and $d_{\min} = 569.52\text{km}$.

Let \hat{i} and \hat{j} be two orthogonal unit vectors in the orbit plane, the position vector of the k th satellite, $k = 0, \dots, N_f - 1$, is

$$\mathbf{r}_k(t) = r_o \left\{ \left[\cos(\omega t) \left(1 - \frac{k^2}{2} \left(\frac{d_{\min}}{r_o} \right)^2 \right) - \sin(\omega t) k \frac{d_{\min}}{r_o} \sqrt{1 - \left(\frac{k}{2} \right)^2 \left(\frac{d_{\min}}{r_o} \right)^2} \right] \hat{i} + \left[\sin(\omega t) \left(1 - \frac{k^2}{2} \left(\frac{d_{\min}}{r_o} \right)^2 \right) + \cos(\omega t) k \frac{d_{\min}}{r_o} \sqrt{1 - \left(\frac{k}{2} \right)^2 \left(\frac{d_{\min}}{r_o} \right)^2} \right] \hat{j} \right\} \mathbf{1},$$

where ω is the orbit angular velocity of the nominal circular orbit

$$\omega = \sqrt{\frac{\mu}{r_o^3}}, \quad (2)$$

and r_o is the orbit radius. The relative position vector from satellite l to satellite k

is given by

$$\begin{aligned} \mathbf{r}_{lk}(t) = d_{\min} \left\{ \left[\cos(\omega t)(l^2 - k^2) \frac{d_{\min}}{2r_o} + \sin(\omega t) \left(-k\sqrt{1 - k^2 \left(\frac{d_{\min}}{2r_o} \right)^2} + l\sqrt{1 - l^2 \left(\frac{d_{\min}}{2r_o} \right)^2} \right) \right] \hat{i} \right. \\ \left. + \left[\sin(\omega t)(l^2 - k^2) \frac{d_{\min}}{2r_o} + \cos(\omega t) \left(k\sqrt{1 - k^2 \left(\frac{d_{\min}}{2r_o} \right)^2} - l\sqrt{1 - l^2 \left(\frac{d_{\min}}{2r_o} \right)^2} \right) \right] \hat{j} \right\}. \end{aligned} \quad (3)$$

In the wave number plane the relative position vector is $\bar{\mathbf{r}}_{lk} = \mathbf{r}_{lk}/\lambda$, a vector emanating from the origin with its tip at the center of the picture frame disc. Ignoring orbit perturbations, the above satellite arrangement guarantees that each $\bar{\mathbf{r}}_{lk}$ has a constant magnitude (since they are distributed along the same circular orbit), which is given by

$$\bar{r}_{lk} = \frac{2r_o\sigma}{\lambda} \sqrt{\left((\hat{l}^2 - \hat{k}^2)\sigma \right)^2 + \left(\hat{k}\sqrt{1 - (\hat{k}\sigma)^2} - \hat{l}\sqrt{1 - (\hat{l}\sigma)^2} \right)^2}, \quad (4)$$

where $\hat{l} = l/(N_f - 1)$, $\hat{k} = k/(N_f - 1)$ ($l, k = 0, 1, 2, \dots, N_f - 1$) and $\sigma = \frac{d_{\max}}{2r_o}$. Note that $0 < \sigma \leq 1$, where $\sigma \rightarrow 0$ as either $d_{\max} \rightarrow 0$ or $r_o \rightarrow \infty$. The latter case arises if the constellation is placed on an orbit with small curvature. As $\sigma \rightarrow 0$ we have $\bar{r}_{lk} \rightarrow d_{\min} |k - l|/\lambda$. $\sigma = 1$ only when $d_{\max} = 2r_o$ (i.e. when the constellation spans 180°). On the other hand, note that for all N_f we have $0 \leq \hat{l}, \hat{k} \leq 1$ and that variations in N_f do not induce variations on \bar{r}_{lk} .

Note that all $\bar{\mathbf{r}}_{lk}$'s rotate at the same (constant) rate, ω , and that this constellation will sweep out the resolution disc in the wave number plane over half an orbit. If the line of sight is tilted away from the orbit normal by an angle ϵ , coverage of the wave number plane will range from full resolution θ_r to a minimum resolution of $\theta_r \cdot \cos \epsilon$. Figure (1) shows the wave number plane coverage for $N_f = 3$. Note that imaging in the opposite direction is possible by rotating the spacecraft 180° about the radius vector.

For the above parameters, the observatory is performing 1.9461×10^{-6} milli-arcsec imaging at $10\mu\text{m}$. Formation keeping and spacecraft pointing of a formation having a maximum baseline of about 14,000km, with a 24pc target and under the influence of J_2 , drag and other perturbations is expected to be a difficult control problem. This may require much tighter pointing requirements than the Hubble Space Telescope. However, note that each aperture in our constellation will probably not be as large as and will not involve as many flexible structures as the Hubble Space Telescope. Moreover, note that since all the spacecraft lie on the same circular orbit, they will all be subject to the same differential perturbations, whose short-term effects are small. Still, these short-term effects can be accounted for by performing accurate relative position measurements between the spacecraft -an issue that is not specific to our observatory, but that is common to a typical interferometric formation.

In summary, Section (1) describes the mapping of wave number plane filling into the motion of N spacecraft in space. Section (2) proposes one way of achieving this mapping in a satisfactory manner. Given this mapping one can seek other motions that achieve the imaging requirements in the wave number plane. Kong et. al.⁴ propose one such motion, where the linearized motion about a circular orbit is considered (thus, Hill’s equations). In their work, the spacecraft are relatively close to each other, allowing for interstellar imaging applications only. Moreover, the imaging region of their “interferometer is limited to only objects that are located in the positive z and positive x directions in the Hill frame”⁴. In contrast, the observatory we propose here provides high resolution imaging of targets that are several parsecs away. More significantly, our observatory does not require any active thrusting to keep the constellation in a near rigid formation.

3 Minimizing the number of satellites for a given resolution

In the fundamental constellation, we define the “fundamental” baselines by $\bar{\mathbf{r}}_{0,k}$ and the “bonus” baselines by $\bar{\mathbf{r}}_{l,k}$, $l \neq 0$. By themselves, the fundamental baselines guarantee complete coverage of the wave number plane over half an orbit period, and the bonus baselines provide redundant coverage. For large N_f , there will be an excessive number of multiple coverage areas, implying that the number of satellites can be reduced with the resolution disc still being completely covered.

To carry out this minimization it is not necessary to consider the two dimensional wave number plane, and is sufficient to consider the one dimensional wave number space. Define a ray in the wave number plane parameterized by the radius $\bar{k}_r \in [0, \bar{k}_{\max}]$, where $\bar{k}_{\max} = 1/(2\theta_r)$. Let the contribution of each pair of satellites (l, k) to the image coverage be given by

$$f_{lk}(\bar{k}_r) = \begin{cases} 1 & \text{if } \bar{k}_r \in [\bar{r}_{lk} - \frac{\bar{d}_{\min}}{2}, \bar{r}_{lk} + \frac{\bar{d}_{\min}}{2}] \\ 0 & \text{otherwise} \end{cases}, \quad (5)$$

for $l = 0, \dots, N - 1$ and $k = l, \dots, N - 1$. Next, define the function $Q(\bar{k}_r) = \frac{1}{N} \sum_{l=0}^{N-1} \sum_{k=l}^{N-1} f_{lk}(\bar{k}_r)$ which is the superposition of all contributions. Figure (1) shows Q for $N = N_f = 3$ ($m = 5$ pixels) and Figure (2) shows Q for $N_f = 16$ ($m = 31$). For the $N_f = 1, 2, 3$ and 4 cases removing any satellite will immediately cause a portion of the resolution disc to not be covered, thus the minimum number of satellites for these cases is $N_{\min}(m) = \frac{1}{2}(m + 1)$. For larger numbers of satellites (i.e., larger number of pixels, m) this is not true.

Our current minimization problem is stated as: “Starting from a fundamental constellation, with a corresponding fixed number of pixels m , maximize the number of satellites that can be removed from the constellation under the constraint that $Q(\bar{k}_r) > 0$ on the interval $\bar{k}_r \in [0, \bar{k}_{\max}]$.” The constraint ensures complete coverage of the wave number line, meaning that each point on the line is covered by at least one

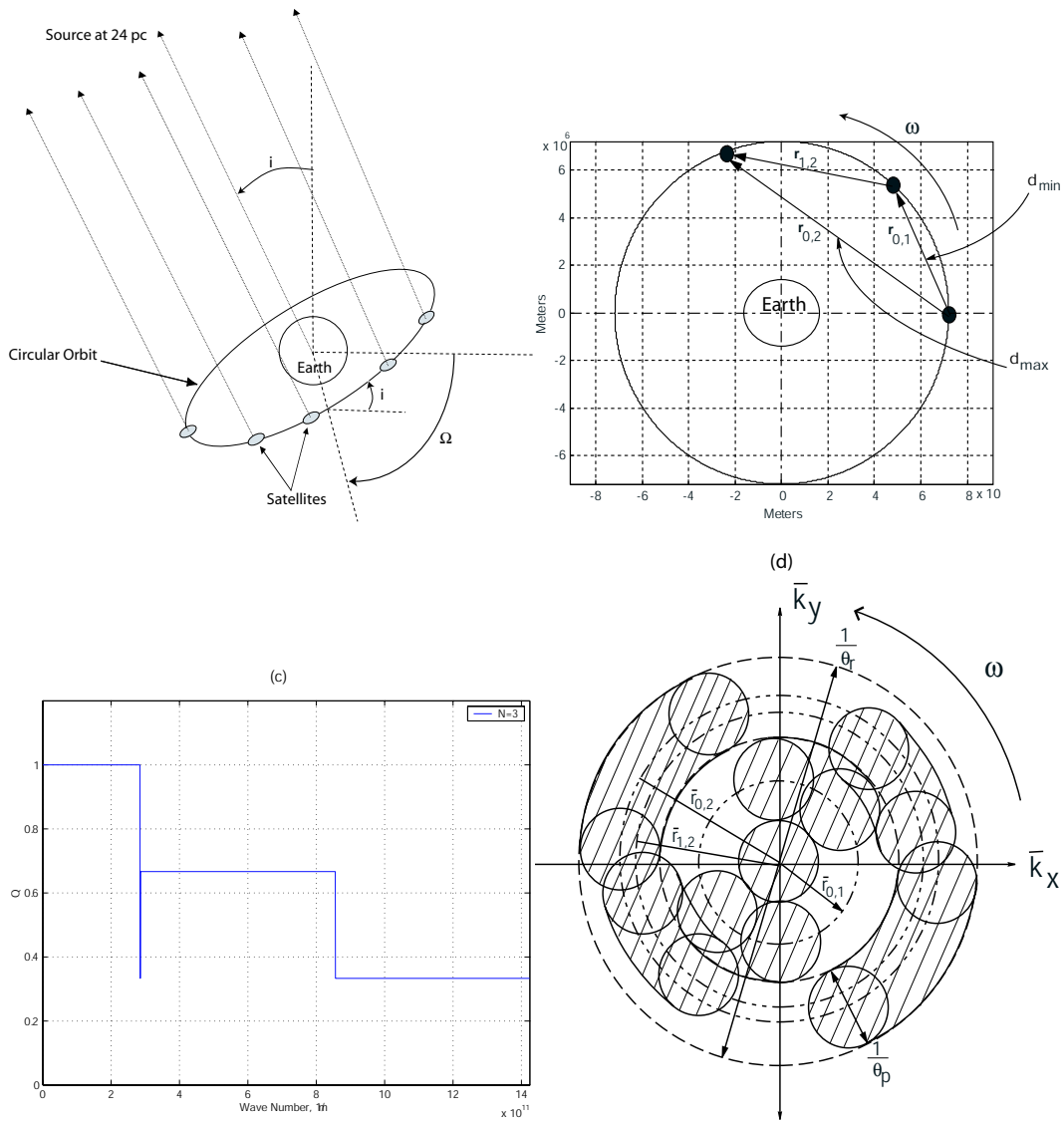


Figure 1: (a) A three dimensional sketch of the imaging observatory (not to scale). (b) Physical distribution in the orbit for $N_f = 3$ (not to scale). (c) Q curve for $N_f = 3$ in the fundamental constellation. (d) Physical distribution in the wave number plane for $N_f = 3, m = 5$ (not to scale).

satellite pair. Satellite arrangements that violate the lower bound are immediately discarded as they will have “gaps” in the wave number line, which lead to spatial frequencies that will not be covered.

To solve this problem, an algorithm was implemented that computes the Q function for the fundamental constellation and all its subsets, found by removing one satellite at a time, two at a time, and so forth. Satellite combinations that violate the lower threshold are discarded and the remaining solutions with a minimum number of satellites, $N_{\min}(m)$, constitute the minimal set. Note that for a given m there may

be several different constellations with the same, minimum, number of satellites.

In a fundamental constellation of N_f satellites, there are up to

$$\sum_{k=1}^{N_f} \binom{N_f}{k} = 2^{N_f} - 1 \quad (6)$$

trials that this algorithm may need to make, for large N_f this is unreasonably large. There are, however, numerous ways to speed up the computation by restricting the space of trials considered, some of which have been used in our computations. This algorithm has been implemented for $m = 3, 5, 7, \dots, 39$, the results summarized in Table (1). Figure (2) shows Q for a fundamental constellation of $N_f = 16$ satellites ($m = 31$ pixels) and a minimum of $N_{\min}(31) = 8$ satellites. The N_{\min} curve shown is the one that maximizes the area under the Q curve over all the 28 possible constellations with 8 satellites, and is comprised of satellites 0, 1, 2, 3, 4, 5, 10 and 15. It is important to note that the minimal sets may change with the factor σ in Eq. (4).

A lower bound on the size of a constellation can be determined as follows. For a constellation of N satellites, there are exactly

$$\binom{N}{2} = \frac{1}{2}N(N-1)$$

baselines. Each baseline provides 2 pixels, plus one for the self pixels giving a total of $m = N(N-1) + 1$. Thus a lower bound on the number of satellites to cover m pixels is given by:

$$N_{lb} = \text{int}^+ \left[\frac{1}{2} (1 + \sqrt{4m-3}) \right],$$

where $\text{int}^+[x]$ is the smallest integer larger than or equal to x . A solution can have no fewer than this number of satellites in the constellation without having gaps in the wave number plane. Moreover, there may not exist solutions with $N_{\min} = N_{lb}$. For example, for $m = 15$ the minimal solution has $N_{\min} = 5$, which is equal to the lower bound. For $m = 29$ the minimal solution has $N_{\min} = 7$, which has one more satellite than the lower bound of 6 (see Table(1)). For large m , the lower bound is approximately $\text{int}^+[\sqrt{m}]$.

4 The Linear Array and its Relation to Earth-Orbiting Constellations

Assume now that we distribute the spacecraft on a linear segment instead of a circular arc (see Figure (3)). There are two ways in which such a situation may arise. The first situation is exemplified by a multi-aperture single spacecraft mission. With the apertures arranged on a line, as opposed to a circular arc, we could still achieve full wave number coverage by a simple 180° rotation of the spacecraft about an axis that is along the line of sight. Since the solution we propose for the LEO observatory hinges

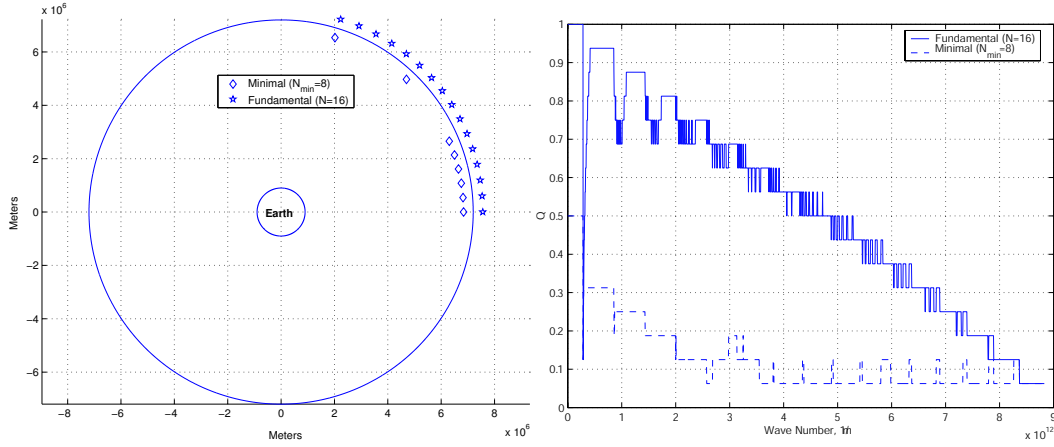


Figure 2: Fundamental and minimal distributions (not to scale) and Q curves for $m = 31$.

Fundamental number of satellites (N_f)	Number of Pixels $m = 2N_f - 1$	Minimum Number of Satellites N_{\min}	Number of Solutions	Lower Bound N_b
1	1	1	1	1
2	3	2	1	2
3	5	3	1	3
4	7	4	1	3
5	9	4	2	4
6	11	5	3	4
7	13	5	3	4
8	15	5	1	5
9	17	6	10	5
10	19	6	3	5
11	21	6	2	5
12	23	7	18	6
13	25	7	12	6
14	27	7	4	6
15	29	7	1	6
16	31	8	28	6
17	33	8	19	7
18	35	8	3	7
19	37	9	142	7
20	39	9	91	7

Table 1: Summary Of Results For A 7200 km Orbit, With $\frac{d_{\min}}{r_o} = 0.0791$ And $\theta_p = 1.75 \times 10^{-11}$

on the assumption that the apertures are rigidly connected and the whole constellation performs a simple rotation about an axis passing through the Earth center, then the concept design proposed above should apply for the linear aperture spacecraft as

well in a space-based short baseline interferometric mission. We may then want to address the same question posed above: how to achieve maximum resolution with the minimum number of satellites and without gaps on the wave number line? For example, University of Michigan’s proposed EV3M⁵ imaging spacecraft is one where all apertures are positioned linearly to maximize the achievable resolution of the spacecraft with three apertures only ($N_f = 4$ spacecraft, $N_{\min} = 3$ spacecraft and $m = 7$ pixels), while fully covering the wave number plane.

Second, note that in the limit as $\sigma \rightarrow 0$, an Earth-orbiting constellation may be approximated, to first order, as a linear array constellation. Thus a solution of the linear constellation will be the same as that for the Earth-orbiting constellation for σ sufficiently small (i.e. either d_{\max} sufficiently small or r_o sufficiently large). As will be shown below, the optimization problem for the linear array can be expressed as a 0-1 mathematical program that can be solved using existing techniques. Techniques, such as evolutionary programming, furnish solutions for high dimensional problems with small computational time, as opposed to exhaustive search algorithms as the one discussed above. This is an advantage in constellation design especially in the case where the constellation contains a very large number of small-sized satellites, where an exhaustive algorithm may take weeks of computation time even on the fastest available computers. Below, the linear array constellation problem will be formulated, solution techniques will be discussed and, in the following section, an application of this solution for an Earth-orbiting array will be discussed.

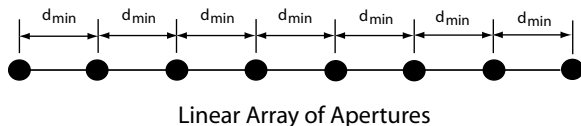


Figure 3: Linear Array Layout

In the “fundamental” arrangement of a linear array of apertures, the relative distance between satellites l and k on the wave number line is given by:

$$\bar{r}_{lk} = |k - l| \frac{d_{\min}}{\lambda}. \quad (7)$$

In Section (2), we parameterized the wave number line by the actual wave number, \bar{k} . Instead, suppose we parameterize it by $\frac{\bar{k}\lambda}{d_{\min}}$. Thus, for the linear constellation, each satellite pair will contribute to a “wave number bin” $[\bar{\chi} - 0.5, \bar{\chi} + 0.5]$ centered at $\bar{\chi}$, where $\bar{\chi} = \frac{\bar{r}_{lk}\lambda}{d_{\min}}$.

Let x_i denote the state of each aperture: x_i is 1 if it is selected as a member of the constellation or 0 if not. So, $x \in \mathbb{B}^{N_f}$, where $\mathbb{B} = \{0, 1\}$ and N_f is the number of satellites in the fundamental set. Note that for a particular choice of apertures, $c^T x$ represents the total number of satellites for that particular choice of apertures, where c is an N_f vector of 1’s.

Next, it can be shown that $b_k(x) = x^T \mathbb{I}_k x$, $k = 1, \dots, N_f$, is equal to the number of contributions to interval number k , where the first interval is centered at the origin

and the N_f th interval is the outermost one and where \mathbb{I}_k is a matrix of zeros except for the $(k - 1)$ st super diagonal. For example, if $N_f = 5$ and satellites 1, 2, 4 are only selected, then the total number of satellites is equal to $[1 \ 1 \ 1 \ 1 \ 1] \cdot [1 \ 1 \ 0 \ 1 \ 0]^T = 3$ satellites. Also, for this case $b_1 = 3$ contributions due to satellites 1, 2 and 4 each paired with itself, $b_2 = 1$ contributions due to the pairing of satellites 1 and 2, $b_3 = 1$ contributions due to pairing of satellites 2 and 4, $b_4 = 1$ contributions due to pairing of satellites 1 and 4 and finally $b_5 = 0$ due to no pairing of satellites which are $5d_{\min}$ apart from each other:

$$\begin{aligned}
b_1 &= [1 \ 1 \ 0 \ 1 \ 0] \begin{bmatrix} 1 & 0 & 0 & 0 & 0 \\ 0 & 1 & 0 & 0 & 0 \\ 0 & 0 & 1 & 0 & 0 \\ 0 & 0 & 0 & 1 & 0 \\ 0 & 0 & 0 & 0 & 1 \end{bmatrix} \begin{bmatrix} 1 \\ 1 \\ 0 \\ 1 \\ 0 \end{bmatrix} = 3, \\
b_2 &= [1 \ 1 \ 0 \ 1 \ 0] \begin{bmatrix} 0 & 1 & 0 & 0 & 0 \\ 0 & 0 & 1 & 0 & 0 \\ 0 & 0 & 0 & 1 & 0 \\ 0 & 0 & 0 & 0 & 1 \\ 0 & 0 & 0 & 0 & 0 \end{bmatrix} \begin{bmatrix} 1 \\ 1 \\ 0 \\ 1 \\ 0 \end{bmatrix} = 1, \\
b_3 &= [1 \ 1 \ 0 \ 1 \ 0] \begin{bmatrix} 0 & 0 & 1 & 0 & 0 \\ 0 & 0 & 0 & 1 & 0 \\ 0 & 0 & 0 & 0 & 1 \\ 0 & 0 & 0 & 0 & 0 \\ 0 & 0 & 0 & 0 & 0 \end{bmatrix} \begin{bmatrix} 1 \\ 1 \\ 0 \\ 1 \\ 0 \end{bmatrix} = 1, \\
b_4 &= [1 \ 1 \ 0 \ 1 \ 0] \begin{bmatrix} 0 & 0 & 0 & 1 & 0 \\ 0 & 0 & 0 & 0 & 1 \\ 0 & 0 & 0 & 0 & 0 \\ 0 & 0 & 0 & 0 & 0 \\ 0 & 0 & 0 & 0 & 0 \end{bmatrix} \begin{bmatrix} 1 \\ 1 \\ 0 \\ 1 \\ 0 \end{bmatrix} = 1, \text{ and} \\
b_5 &= [1 \ 1 \ 0 \ 1 \ 0] \begin{bmatrix} 0 & 0 & 0 & 0 & 1 \\ 0 & 0 & 0 & 0 & 0 \\ 0 & 0 & 0 & 0 & 0 \\ 0 & 0 & 0 & 0 & 0 \\ 0 & 0 & 0 & 0 & 0 \end{bmatrix} \begin{bmatrix} 1 \\ 1 \\ 0 \\ 1 \\ 0 \end{bmatrix} = 0.
\end{aligned}$$

Because $b_5 = 0$, $x = [1 \ 1 \ 0 \ 1 \ 0]^T$ is not a solution to the problem.

Thus the set of designs with the minimum number of satellites that completely cover the wave number line are all *global* solutions to the following minimization problem:

$$\begin{aligned}
&\min_x c^T x \\
&\text{s.t. } b_k(x) \geq 1, \quad k = 1, \dots, N_f \\
&\quad x \in \mathbb{B}^{N_f}.
\end{aligned} \tag{8}$$

This problem is generally known in the literature as a combinatoric/integer 0-1 programme, usually with linear cost function and linear constraints⁶. The solution of this problem requires the minimization of a linear cost function subject to a quadratic constraint. General 0-1 programming techniques exist to solve the program in Eq. (8).

4.1 Numerical Results

We first attempt to solve this problem by applying a thorough search algorithm as discussed in previous Section (3). Figure (4) shows the number of feasible solutions (top left), the number of minimal solutions (top right), N_{\min} (bottom left) and the CPU time (using a 1.5GHz IBM platform) in hours (bottom right). The advantage of this algorithm is that it gives complete information on all possible minimal solutions (e.g. the configuration of spacecraft in each solution). The main drawback is the computational time involved to obtain the results. For example, for $N_f = 21$ spacecraft there are 2.5×10^5 feasible solutions that all require evaluation of their Q functions, consuming about 7 hours using the exact search algorithm.

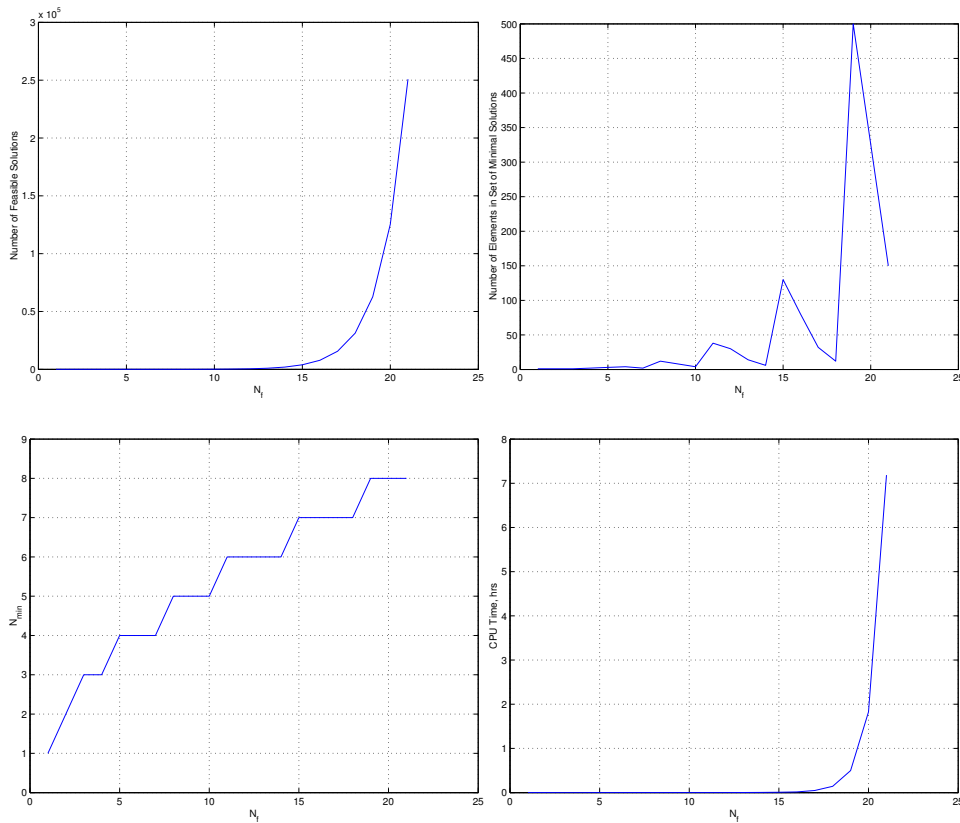


Figure 4: Exact Search Algorithm Results

To decrease the amount of CPU time, a statistical approach to solving the above 0-1 program is to utilize an evolutionary programming (EP) method. This is schemat-

ically summarized in Figure (5). The results of applying this algorithm are shown in Figure (6). We notice a tremendous amount of computation time savings. Using this algorithm we can arrive at solutions in about 11 seconds for $N_f = 21$ spacecraft. Due to the random nature of the search algorithm of the EP method, we note that we do not have full information regarding the total number of solutions available, the size of the feasible set or the exact design of the constellation (i.e. we may only know what N_{\min} is, but not the full set of solutions that achieves N_{\min} spacecraft).

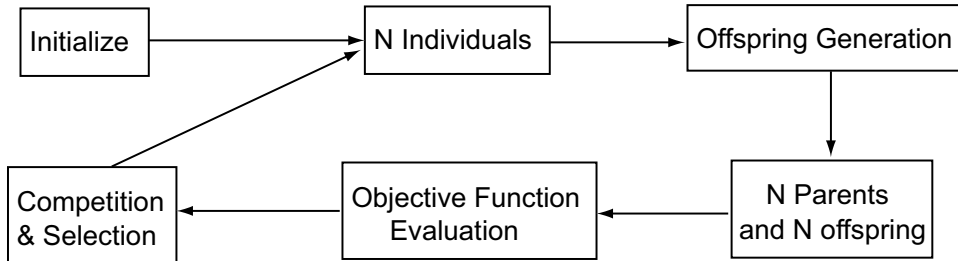


Figure 5: An Evolutionary Programming Method

A closer look at the right hand plot in Figure (6) shows that we seem to be able to get the correct solution up to $N_f = 32$. However, for $N_f = 37$ we notice a drop in N_{\min} . Since it is not possible for a larger fundamental constellation (that achieves higher resolution) to achieve a smaller N_{\min} than a smaller fundamental constellation, then we know that the N_{\min} obtained using the EP algorithm for $N_f = 37$ is not correct. This result casts larger doubt that the results obtained for $N_f > 37$ will be correct either, though we could be confident that results for values of $N_f \leq 36$ seem to be plausible.

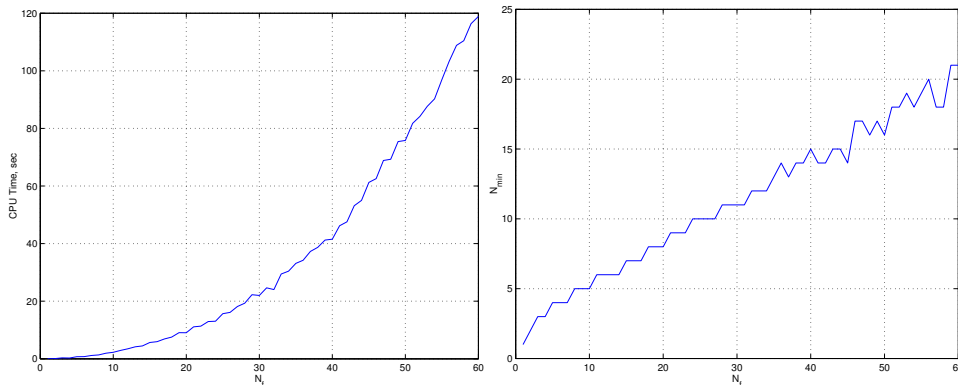


Figure 6: EP Algorithm Results

We observe that the algorithm performs poorly for higher values of N_f , though it is much faster than the exact search algorithm. In general one would trade off accuracy of solutions for speed in an EP algorithm. One may wish to improve the results, though at the expense of longer computational time, by constricting the

offspring generated to be ones that are visible in the first place. The results are shown in Figure (7), where we observe that consistent results are obtained for values of $N_f \leq 23$. For $N_f = 23$, the computation time is 1.8 hours versus 18 seconds for the general EP algorithm and more than 7 hours for the thorough search algorithm.

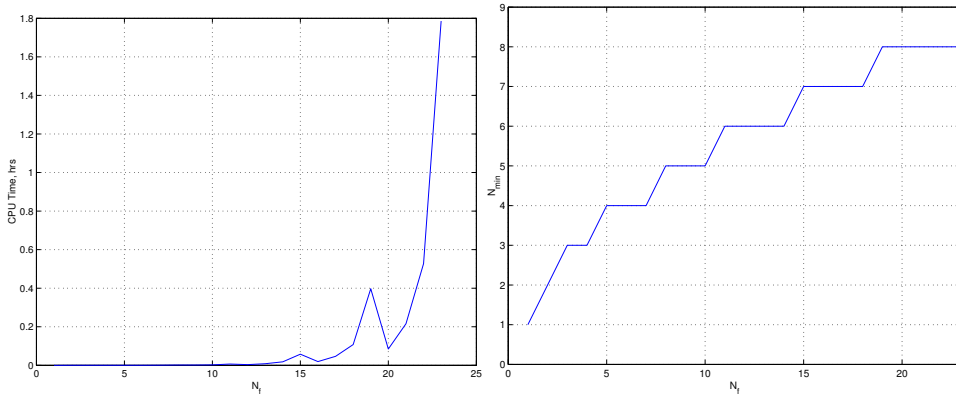


Figure 7: Restricted EP Algorithm Results

4.2 The Linear Array and the Earth-Orbiting Observatory

Assume that we can find a distance preserving isometry, ϕ , between the (curved) Earth-orbiting and the linear array geometries discussed above. As mentioned above, the significance of the linear problem is that we can readily solve this problem (as stated in Eq. (8)) and then compute the corresponding solution on the curved one-dimensional space through the inverse mapping ϕ^{-1} (see Figure (9)). The main benefit is that we can utilize techniques available in the literature for solving the 0-1 program in Eq. (8) to compute the solution to an Earth-orbiting configuration. First, recall the definition for an isometry and isometric spaces⁷:

Definition 4.1 (Isometry and Isometric Spaces) *Let M_1 and M_2 be two topological spaces. An isometry $\phi : M_1 \rightarrow M_2$ is a one-to-one correspondence such that $d_2(\phi(x), \phi(y)) = d_1(x, y)$ for all $x, y \in M_1$, where $d_1(\cdot, \cdot)$ and $d_2(\cdot, \cdot)$ are distance functions on M_1 and M_2 , respectively. If there exists an isometry $\phi : M_1 \rightarrow M_2$, then M_1 and M_2 are called isometric.*

S^1 being the circle in \mathbb{R}^2 with radius r_o , let $M_C \subset S^1$ denote the one-dimensional space for a curved Earth-orbiting constellation and $M_L \subset \mathbb{R}^1$ be the one-dimensional space, which is simply a line segment on \mathbb{R}^1 , for the linear aperture constellation.

Let $d_C(s_l, s_k)$ be the Euclidean distance in \mathbb{R}^2 between satellites k and l on M_C and let $d_L(s_l, s_k)$ be the Euclidean distance in \mathbb{R}^1 between satellites k and l on M_L . d_C and d_L are given by

$$d_C(s_l, s_k) = \frac{2r_o\sigma}{\lambda} \sqrt{\left((\hat{l}^2 - \hat{k}^2)\sigma\right)^2 + \left(\hat{k}\sqrt{1 - (\hat{k}\sigma)^2} - \hat{l}\sqrt{1 - (\hat{l}\sigma)^2}\right)^2} \quad (9)$$

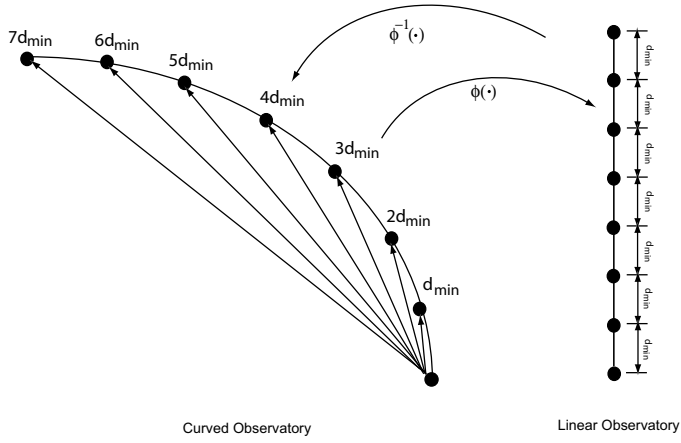


Figure 8: Relation between the Linear And Earth-Orbiting Constellations

where \hat{l} and \hat{k} are as defined in Section (2), and

$$d_L(s_l, s_k) = |k - l| d_{\min}/\lambda \quad (10)$$

Due to the way spacecraft are arranged in the fundamental configuration, M_C and M_L may not have an isometry. That is because if M_C is simply unfolded onto M_L , spacecraft nodes on M_C do not map onto spacecraft nodes on M_L . Though it is true that the real line \mathbb{R}^1 and the circle S^1 have the isometry $\phi(t) = (r_o \sin t, r_o \cos t) : \mathbb{R}^1 \rightarrow S^1 \subset \mathbb{R}^2$ using a metric that measures distance *along* the curves, this is not true in our case because the metric we must use for imaging is the direct shortest distance between points in \mathbb{R}^2 as opposed to a metric along S^1 .

For $\sigma \neq 0$, points on $M_C \subset S^1$ are shifted when M_C is unfolded onto M_L . Despite the fact that the total distance from the zeroth spacecraft to the $(N_f - 1)^{\text{st}}$ spacecraft is preserved and is equal to d_{\max} , distances between intermediate spacecraft are not.

It can be shown that:

$$d_C(s_l, s_k) = \frac{2r_o\sigma}{\lambda} \left| \hat{k} - \hat{l} \right| + O(\sigma^3) = d_L(s_l, s_k) + O(\sigma^3).$$

Hence, we have:

$$\lim_{\sigma \rightarrow 0} d_C(s_l, s_k) = d_L(s_l, s_k). \quad (11)$$

In other words, $d_C(s_l, s_k) \rightarrow d_L(s_l, s_k)$ as the curvature of M_C or d_{\max} approach zero. Thus, to a first order approximation, distance is conserved under the isometry $\phi(t) = (r_o \sin t, r_o \cos t)$ and the solution to the linear array should be identical to that of the curved array. In the next section we show results that indicate that for sufficiently small σ , the solution to the mathematical program in Eq. (8) is also a solution to the Earth-orbiting constellation configuration. On the other hand, note that since $0 \leq \hat{l}, \hat{k} \leq 1$, N_f will not have variational effects on the solution. Thus, one only needs to take into consideration variations in σ when seeking solutions to the Earth-orbiting constellation that are based on solutions to the linear array.

4.3 Numerical Results

In this section, we solve (8) using an exact search algorithm and compare the result with those obtained for a curved constellation. The results show that the two solutions indeed match, as predicted, for all values of σ small and up to a critical value σ^* . For $\sigma > \sigma^*$, the solution to the Earth-orbiting constellation deviates from that obtained for the linear array. For instance, for $N_f = 9$, the algorithm finds 8 minimal solutions to the linear array, whereas for the curved constellation it finds only 6 for $\sigma = \sigma^* = 0.019$. Figure (9) shows a plot for σ^* as a function of N_f for $5 \leq N_f \leq 10$. Note that for $1 \leq N_f \leq 4$, there exists just a single minimum and, thus, σ^* is undefined there.

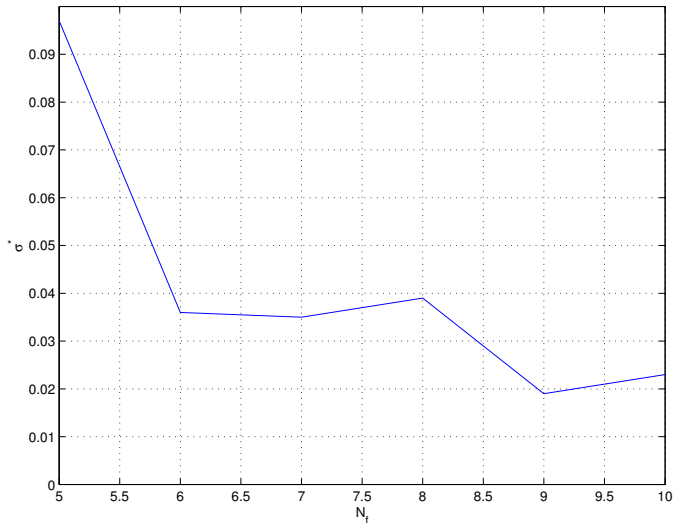


Figure 9: σ^* For $5 \leq N_f \leq 10$

5 The Interferometric Observatory

The Earth-orbiting constellation configurations proposed above will completely cover the wave number plane in half an orbit period, while imaging for several orbital periods will result in improved image quality. Thus, over a short period (days at most) an image can be formed. If we place the constellation in an inclined orbit, the orbit plane will precess relative to inertial space due to J_2 and the constellation will scan across the celestial sphere at a constant rate, effectively repeating its coverage after half a nodal period. The precession rate of the orbit plane is given by⁸

$$\dot{\bar{\Omega}} = -\frac{3}{2} \sqrt{\frac{\mu}{r_o^3}} \frac{R_o^2 J_2}{r_o^2} \cos(i),$$

where $R_o = 6378.14\text{km}$ is the Earth's radius, $J_2 = 0.00108263$ is the second zonal harmonic of the Earth, $\mu = 3.986005 \times 10^5 \text{km}^3/\text{s}^2$ is the Earth's gravitational constant,

i is the inclination, r_o is the orbital radius, and the precession period of the node is $T = \frac{2\pi}{\dot{\Omega}}$. For an 800km altitude orbit inclined at 45° to the equator, the precession period is 77 days. For a constellation in a 45° or 135° inclination orbit, every point on the celestial sphere can be imaged with a resolution ranging from θ_r to $\theta_r/\sqrt{2}$ within half a nodal period.

An important design consideration is the speed at which the picture frame disc moves in the wave number plane, as this affects the image quality. The larger this speed is, the poorer the image quality becomes. Given an upper bound on the wave-plane velocity, \bar{v} , and a desired angular resolution, θ_r , this constrains the angular rate at which the picture frame disc moves in the wave number plane, equal to the mean motion of the orbit, $\omega \leq \frac{1}{2}\bar{v}\theta_r$. This bounds the desired orbit radius, $r_o \geq \sqrt[3]{\frac{4\mu}{(\bar{v}\theta_r)^2}}$. Thus, the choice of orbit radius does not depend only on the desired baselines (determined from the desired angular resolution), but also on the desired image quality. Note that it is possible to trade a higher speed in the wave number plane (shorter period) with additional observations, striking a balance between the two.

Other issues of concern are the signal detection, transmission and interference. There are certain optical technologies that are assumed to exist for this proposed very long baseline LEO observatory to be feasible. We assume that either a heterodyne or a direct detection method is used. Heterodyne detection has the advantage of selecting and detecting only the components of the wavefront of the source that are in phase with the wavefront of a local laser oscillator⁹. Thus, heterodyne detection furnishes phase information. On the other hand, direct detection, though less efficient as far as signal to noise is concerned, is still feasible via spatial filtering with a glass fiber to obtain a single geometric mode¹⁰. Local heterodyne detection, however, has a major advantage over direct detection Michelson interferometry. Direct detection requires that the detected signal be divided into $N - 1$ equal parts, where N is the number of satellites in the constellation, corresponding to $N - 1$ baselines. This results in the reduction of the signal by a factor of $N - 1$. Each of the $N - 1$ signals will possess a reduced SNR. This is exacerbated due to the presence of large background noise and the long distances over which the signals are transmitted from each spacecraft to a combiner spacecraft. For wavelengths above $\sim 4\mu\text{m}$, heterodyne detection is likely to be superior because of these problems with direct detection. It could be shown, however, that below $\sim 4\mu\text{m}$, direct detection will have better SNR properties than heterodyne detection. For a $10\mu\text{m}$ mission, such as the one proposed in this paper, heterodyne detection is advantageous.

A technique different from heterodyne detection is also under investigation by our group. This is Fourier Transform Spectral Interferometry for electric field reconstruction in a separated spacecraft interferometric mission. Novel optical techniques exist, such as Dual-Quadrature Spectral Interferometry (DQSI) and Spectral Phase Interferometry for Direct Electric Field Reconstruction (SPIDER), that aim at the full characterization of an electric field, both temporally and spatially^{11,12}. The goal of such research, which has so far been developed for highly coherent sources and is currently being developed for non-coherent sources, is to extract necessary informa-

tion in digital form that allow for performing the interference process digitally on a microchip. Once such digital information is available, these can be sent via communication links such as radio frequency signals to a central processing unit located on one of the spacecraft for the mutual intensity computations and metrology measurements. In light of technologies such as heterodyne detection or electric field reconstruction, a very long baseline mission such as the one we propose in this paper should be feasible as far as the optics are concerned.

A final remark is that JPL's Terrestrial Planet Finder (TPF) technology is an IR interferometer that currently does not involve baselines longer than 100m between apertures. TPF may provide an angular resolution that is as small as 0.75 milli-arcsec at $3\mu\text{m}$ and 1000m baseline. This corresponds to single pixel detection of a planet located 0.5AU from a sun-like star¹³. The main aim of TPF is to detect an earth-like planet by separating the planet from its parent star and capturing its light on a single pixel. In contrast, the underlying aim of the proposed observatory is to form a multi-pixel image of the disk of the planet. In consequence, the very long baseline constellation, such as the example we use here, offers 1.9461×10^{-6} milli-arcsec resolution at $10\mu\text{m}$ and a longest baseline of over 14,000km.

6 Conclusion

In this paper, the imaging objectives are stated and a class of constellations that can achieve high resolution images in LEO was discussed. An optimization procedure is also defined that supplies m pixels of resolution with a minimum number of satellites. We introduced a linear imaging constellation and formulated a 0-1 mathematical program, the solution of which is the solution to the optimal aperture configuration for full coverage of the wave number plane. This, in turn, helps to numerically solve the constellation design problem for a general Earth-orbiting constellation. We discussed how the zonal J_2 effect can be utilized to scan the observatory across the celestial sphere. Finally, we discussed some practical implementation issues. Future research will study the behavior of similar constellations subject to more general gravitational fields.

References

- [1] M. Born and E. Wolf. *Principles of optics*, Pergamon Press, New York, 1964.
- [2] D. C. Hyland. Interferometric Imaging Concepts With Reduced Formation-Keeping Constraints. *AIAA Space 2001 Conference*, Albuquerque, NM, August, 2001.
- [3] D. C. Hyland. Formation Control for Optimal Image Reconstruction in Space Imaging Systems. *International Symposium on Formation Flying*, October 29-31, Centre National d'Etudes Spatiales, Toulouse, France.

- [4] E. M. C. Kong, D. W. Miller and R. J. Sedwick. Exploiting Orbital Dynamics for Interstellar Separated Spacecraft Interferometry. *Proceedings of the American Control Conference*, pp. 4153-4157, 1999.
- [5] S. E. Gano et. al. A Baseline Study of a Low-Cost, High-Resolution, Imaging System Using Wavefront Reconstruction. *AIAA Space 2001 Conference*, Albuquerque, NM, August, 2001.
- [6] Y. J. Cao, L. Jiang and Q. H. Wu. An Evolutionary Programming Approach to Mixed-Variable Optimization Problems. *Applied Mathematical Modelling*, Vol. 24, pp. 931-942, 2000.
- [7] W. A. Sutherland. *Introduction to Metric and Topological Spaces*, Oxford Science Publications, Oxford, 1975.
- [8] A. E. Roy. *Orbital Motion*, 3rd ed., Institute of Physics Publishing, Philadelphia, 1998.
- [9] H. Townes. Noise and Sensitivity in Interferometry. Chapter 4 of *Principles of Long Baseline Interferometry*. Course Notes from the 1999 Michelson Summer School, August 15-19, 1999, P. Lawson, Ed. JPL Publication 00-009, July 2000.
- [10] R. H. Kingston. Detection of Optical and Infrared Radiation. *J. Oppt. Soc. Am. B.*, Vol. 4, 1450-1741, 1978.
- [11] L. Lepetit, G. Chriaux, and M. Joffre. Linear Techniques of Phase Measurement by Femtosecond Spectral Interferometry for Applications in Spectroscopy. *J. Opt. Soc. Am. B.*, Vol. 12, No. 12, December 1995.
- [12] C. Iaconis and I. Walmsley. Self-Referencing Spectral Interferometry for Measuring Ultrashort Optical Pulses. *IEEE J. of Quantum Mechanics*, Vol. 35, No. 4, April 1999.
- [13] *The Terrestrial Planet Finder: A NASA Origins Program to Search for Habitable Planets*. JPL Publication 99-003, May 1995.